



# Thioredoxin-80 protects against amyloid-beta pathology through autophagic-lysosomal pathway regulation

Gorka Gerenu <sup>1,2,3</sup> · Torbjörn Persson <sup>1</sup> · Julen Goikolea<sup>1</sup> · Javier Calvo-Garrido<sup>1</sup> · Raúl Loera-Valencia <sup>1</sup> · Philipp Pottmeier<sup>1</sup> · Cesar Santiago <sup>4</sup> · Helen Poska<sup>1,5</sup> · Jenny Presto<sup>1</sup> · Angel Cedazo-Minguez <sup>1</sup>

Received: 31 January 2019 / Revised: 2 July 2019 / Accepted: 2 August 2019 / Published online: 13 September 2019  
© The Author(s), under exclusive licence to Springer Nature Limited 2019

## Abstract

Aggregation and accumulation of amyloid beta (A $\beta$ ) are believed to play a key role in the pathogenesis of Alzheimer's disease (AD). We previously reported that Thioredoxin-80 (Trx80), a truncated form of Thioredoxin-1, prevents the toxic effects of A $\beta$  and inhibits its aggregation in vitro. Trx80 levels were found to be dramatically reduced both in the human brain and cerebrospinal fluid of AD patients. In this study, we investigated the effect of Trx80 expression using in vivo and in vitro models of A $\beta$  pathology. We developed *Drosophila melanogaster* models overexpressing either human Trx80, human A $\beta$ <sub>42</sub>, or both A $\beta$ <sub>42</sub>/Trx80 in the central nervous system. We found that Trx80 expression prevents A $\beta$ <sub>42</sub> accumulation in the brain and rescues the reduction in life span and locomotor impairments seen in A $\beta$ <sub>42</sub> expressing flies. Also, we show that Trx80 induces autophagosome formation and reverses the inhibition of Atg4b-Atg8a/b autophagosome formation pathway caused by A $\beta$ <sub>42</sub>. These effects were also confirmed in human neuroblastoma cells. These results give insight into Trx80 function in vivo, suggesting its role in the autophagosome biogenesis and thus in A $\beta$ <sub>42</sub> degradation. Our findings put Trx80 on the spotlight as an endogenous agent against A $\beta$ <sub>42</sub>-induced toxicity in the brain suggesting that strategies to enhance Trx80 levels in neurons could potentially be beneficial against AD pathology in humans.

These authors contributed equally: Gorka Gerenu, Torbjörn Persson

**Supplementary information** The online version of this article (<https://doi.org/10.1038/s41380-019-0521-2>) contains supplementary material, which is available to authorized users.

- ✉ Gorka Gerenu  
gorka.gerenu@biodonostia.org
- ✉ Angel Cedazo-Minguez  
Angel.Cedazo-Minguez@ki.se

- <sup>1</sup> Center for Alzheimer Research, Division of Neurogeriatrics, Department of Neurobiology, Care Sciences and Society, Karolinska Institutet, Bioclinicum J9:20, Solnavägen 30, 171 64 Solna, Sweden
- <sup>2</sup> Biodonostia Health Research Institute, Neuroscience Area, 20014 Donostia-San Sebastián, Gipuzkoa, Spain
- <sup>3</sup> CIBERNED (Network Center for Biomedical Research in Neurodegenerative Diseases), Carlos III Institute, Madrid, Spain
- <sup>4</sup> National Centre for Biotechnology, CSIC; Macromolecular Structures Department, 28049 Madrid, Spain
- <sup>5</sup> School of Natural Sciences and Health, Tallinn University, Narva mnt 29, 101 20 Tallinn, Estonia

## Introduction

Alzheimer's disease (AD) is the main cause of dementia in the elderly. Current AD treatments are only able to delay the cognitive decline of patients, but not to cure the disease [1]. AD and other neurodegenerative diseases share some associated pathologies as synaptic dysfunction and accumulation of toxic proteins [2]. The main hallmarks of AD brains are intracellular neurofibrillary tangles and extracellular neuritic plaques [3], the latter mainly composed of amyloid fibrils of misfolded amyloid-beta (A $\beta$ ) peptides [4]. These A $\beta$  peptides are believed to contribute importantly to the disease pathogenesis and to have neurotoxic effects. A $\beta$  is generated when the two transmembrane proteases  $\beta$ - and  $\gamma$ -secretase sequentially cleave the amyloid precursor protein (APP) [5]. An alternative cleavage by  $\alpha$ -secretases is dominant in healthy neurons and does not generate A $\beta$  peptides [6].

The endogenous dithiol reductant Thioredoxin-1 (Trx1) is an evolutionarily highly conserved protein with many different roles, from scavenging of reactive oxygen species to chemokine activities [7]. This protein can be truncated, generating an 80 amino acid long peptide called

Thioredoxin-80 (Trx80). The peptide lacks antioxidant capacity [8] and its role remains elusive even though it was primarily described as a chemokine [9].

In addition to the non-amyloidogenic cleavage of APP, we have previously found evidence that two  $\alpha$ -secretases, ADAM10 and 17, are also responsible for the Trx1 proteolytic cleavage that generates Trx80. We also demonstrated that Trx80 prevents amyloid formation of  $A\beta_{42}$  and inhibits its toxic effects in cellular models [10]. Moreover, the levels of Trx80 are decreased in brain homogenates and in cerebrospinal fluid of patients with AD compared with matched controls [10]. These results suggest a protective role of Trx80 against  $A\beta_{42}$  effects and therefore on AD pathology. However, the Trx80 effects in vivo and the underlying mechanism need to be identified.

We have generated a new model of *Drosophila melanogaster* that overexpresses human Trx80 exclusively in the brain. To analyze Trx80 effects on  $A\beta_{42}$  accumulation and  $A\beta_{42}$ -induced reduction of life span and locomotor capabilities, these flies were crossed with the previously characterized human  $A\beta_{42}$  overexpressing flies [11]. In the present study, we found that Trx80 overexpression leads to a reduction of  $A\beta_{42}$  levels in the brain and protects against  $A\beta_{42}$  induced phenotypes. Moreover, Trx80 overexpression resulted in the induction of the autophagic-lysosomal degradation pathway in the brain. Similar effects were also found in-vitro in human neuroblastoma cells (SH-SY5Y cells), suggesting that these effects are conserved in different evolutionary stages.

## Material and methods

### Transgenic *Drosophila melanogaster*

Transgenic Trx80-overexpressing *Drosophila* strain: human Trx80 cDNA sequence was cloned into pUASTattB vector and PhiC31 integrase system (BestGene Inc.) was used for transgenesis to the 86F8 locus at third chromosome. h $A\beta_{42}$  overexpressing fly was provided by Gunilla Westermark (Uppsala University) [12]. The experimental approach was based on UAS-Gal4 expression system, using the pan-neuronal *elav*<sup>c155</sup>-Gal4 (Fig. 1a) *Drosophila melanogaster* driver strain [13]. W1118 wild-type flies crossed with *elav*<sup>c155</sup> were used as control flies. Female flies were used in the experiments. Flies were housed at 24 °C, 70% humidity and 12 h/12 h light/darkness cycle.

### Longevity assay

One hundred flies (five females per tube) were selected from each strain. Dead flies were counted every 2 days. Kaplan–Meier method was used to plot the results. A log-rank

test was used to analyze results and Bonferroni correction for multiple comparisons.

### Locomotor activity

Twenty-days-old flies were analyzed in groups of five. They were placed in a tube with an 8 cm mark from the bottom. Assays were recorded and archived. The number of flies that passed the 8 cm mark in 10 s was counted (5 times/tube).

### Trx80 and Trx1 overexpressing-SH-SY5Y cells: DNA constructs and transfection

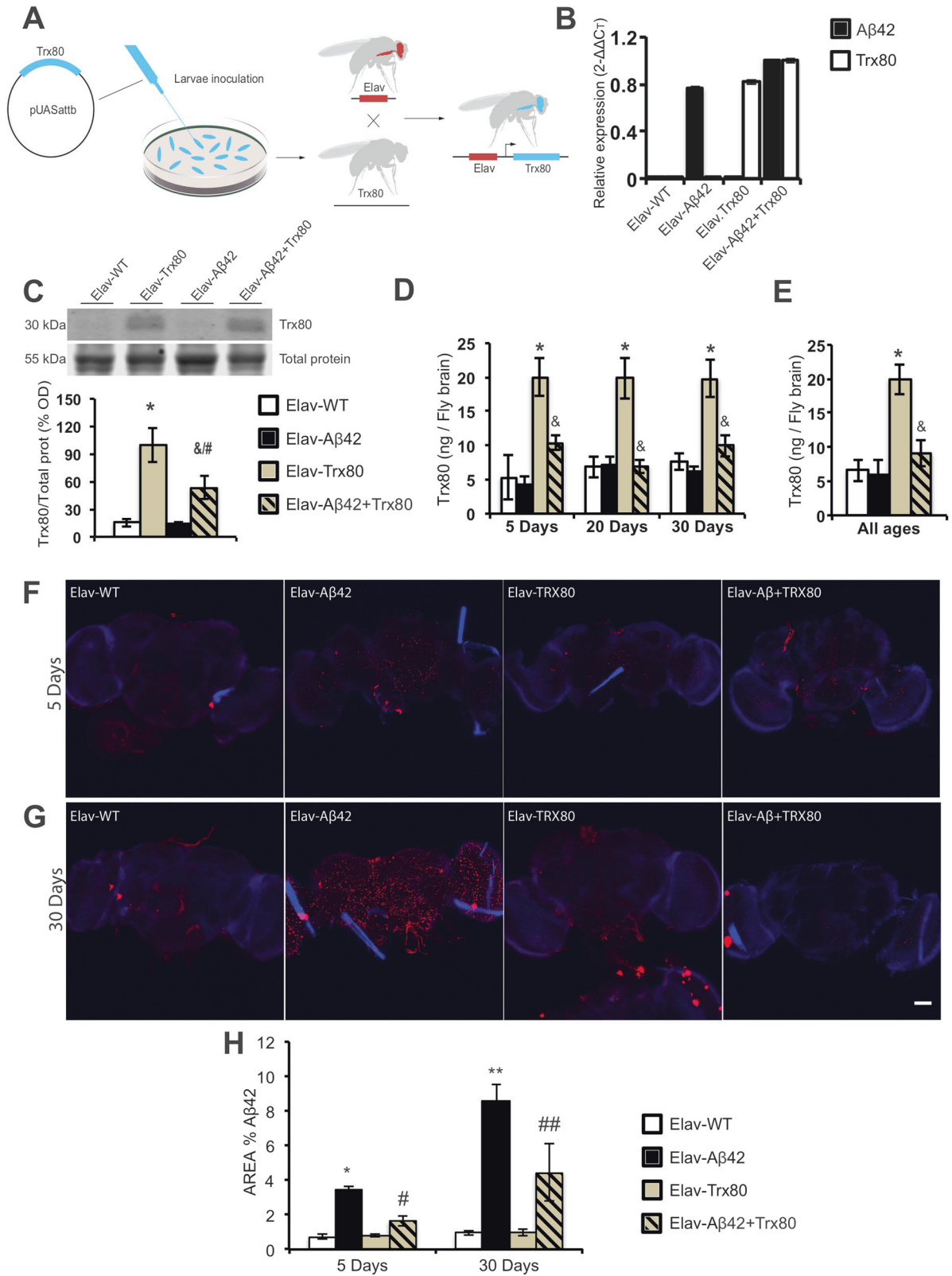
The Trx1 plasmid used was generated previously. Based on Trx1 plasmid, we reproduced the method to overexpress Trx80 [10]. Following forward (5′CGAATTCGCCACCA TGGATTACAAGGATGACGACGATAAGATGGTGAA GCAGATCGAG-3′ and reverse (5′CGGATCCTTACTT AAAAACTGGAATGTTGGCATGCATTT-GACTTCA C-3) primers were used.

### Cell line cultures and treatments

Control SH-SY5Y empty vector and SH-Trx80 cells were cultured in DMEM/F12 with FBS (10%) and Geneticin (Invitrogen), incubated at 37 °C and 5% CO<sub>2</sub>. Treatments: 50 mM ammonium chloride (2 h) (NH<sub>4</sub>Cl) (Sigma-Aldrich). 30  $\mu$ M Chloroquine (CQ) (Sigma-Aldrich) or 200 nM Epoxomicin (EPOX, Selleckchem) treatment or vehicle for 6 h. Pre treatment: 500 nM recombinant Amyloid-beta protein fragment 1–42 ( $A\beta_{42}$ ) (Sigma-Aldrich) for 16 h.

### Sample preparation and western blot

Ten fly brains were obtained to measure protein levels by western blot of flies. For APP-derived fragments, the homogenization was performed in Tris-HCl-SDS 1% buffer and centrifuged at 100,000  $\times$  g 1 h. Blots were performed as previously described [10]. Briefly, proteins were extracted in RIPA buffer containing phosphatase and protease inhibitors (Sigma-Aldrich). Homogenates were centrifuged at 14000  $\times$  g for 20 min 4 °C (except for amyloid beta detection, 100,000  $\times$  g, 1 h 4 °C). All samples were mixed with an equal volume of loading buffer (0.16 M Tris-HCl pH 6.8, 4% SDS, 20% glycerol, 0.01% bromophenol blue, 0.1 M DTT) and ran in Tris-HCl gels (Tris-tricine for amyloid beta). Proteins were transferred to BioTrace™ Nitrocellulose membranes (GE healthcare) (PVDF for amyloid beta) overnight 4 °C at 20 V. After 1 h blocking in 5% BSA TBS-T, Membrane was incubated with specific primary antibodies overnight 4 °C. Primary Antibodies: ATG-4B (1:1000, Sigma-Aldrich); Atg12 (1:1000, #4180, Cell



Signaling) anti-ATG8 (1:1000, #ABC974 Millipore); SQSTM1/p62 (1:2000, #5114, Cell signaling); LC3B (1:1000, #2775, Cell Signaling); Trx1 (1:1000, Trx1-03,

IMCO), Trx80 (1:1000, 7D11, IMCO), Draper (5D14) (1:250, DSHB), phospho-AMPKα (Thr172)(1:1000, #2535, Cell Signaling), total AMPKα (1:2000, #2532, Cell

◀ **Fig. 1** A $\beta_{42}$  levels are decreased by Trx80 overexpression in vivo in a *Drosophila melanogaster* model for Alzheimer's Disease. **a** Schematic illustration describing the generation of the Trx80 expressing *D. melanogaster* strain using the  $\phi$ C31 system (BestGene, USA) and the *elav<sup>c155</sup>*-GAL4 driver strain to obtain pan-neuronal expression. **b** Levels of Trx80 and A $\beta_{42}$  mRNAs in head homogenates from 10-day-old flies. The levels are compared with the levels in flies expressing both Trx80 and A $\beta_{42}$ . **c** Representative Trx80 blot of all four fly genotypes and Trx80 blot quantification. Data are normalized to total protein staining and are presented as percentage of values for WT. Results are expressed as mean  $\pm$  SD. Statistical analysis was performed by two-way ANOVA ( $*p < 0.01$ ) and Bonferroni multiple comparisons A $\beta_{42}$  vs A $\beta_{42}$ /Trx80 ( $\&p < 0.01$ ), WT vs A $\beta_{42}$ /Trx80 ( $\#p < 0.05$ ) ( $n = 3$ ). **d** Age-dependent progression in Trx80 protein levels was measured by specific sandwich ELISA at 5, 20, and 30-day-old flies. Trx80 is presented as ng per fly brain. Results are expressed as mean  $\pm$  SD. Statistical analysis was performed by two-way ANOVA ( $*p < 0.01$ ) and Bonferroni multiple comparisons (A $\beta_{42}$  vs A $\beta_{42}$ /Trx80,  $\&p < 0.01$ ) ( $n = 3$ ). **e** Age-independent Trx80 ELISA measurement (average of all ages) for all four groups presented as ng per fly brain. Results are expressed as mean  $\pm$  SD. Two-way ANOVA ( $*p < 0.01$ ) and Bonferroni multiple comparison (A $\beta_{42}$  vs A $\beta_{42}$ /Trx80,  $\&p < 0.01$ ) was performed ( $n = 3$ ). **f** A $\beta_{42}$  deposition is lower in 5-day-old fly brains of A $\beta_{42}$ /Trx80 co-expressing flies compared with A $\beta_{42}$  transgenic flies. Representative merged images of A $\beta_{42}$  and DAPI staining in 5-day-old fly brains of all genotypes. Scale bar represents 50  $\mu$ M. ( $n = 5$ ) **g** A $\beta_{42}$  deposition is dramatically reduced in 30-day-old fly brains of A $\beta_{42}$ /Trx80 co-expressing flies compared with A $\beta_{42}$  transgenic flies. Representative merged image of A $\beta_{42}$  and DAPI staining in 30-day-old fly brains of all genotypes. Scale bar represents 50  $\mu$ M. **h** Bar graph showing the quantification of area % stained with anti-A $\beta_{42}$  antibody (JNKI) for all groups. Results are expressed as mean  $\pm$  SD. Two-way ANOVA ( $*p < 0.05$ ;  $**p < 0.01$ ) was performed and Bonferroni multiple comparison (A $\beta_{42}$  vs A $\beta_{42}$ -Trx80,  $\#p < 0.05$ ,  $\#\#p < 0.01$ ,  $n = 5$ )

signaling), and Tubulin (1:10000, T9026, Sigma). Either HRP (cell signaling) or fluorescent secondary antibodies were used at 1/10,000, 2 h, RT. Bands were visualized and quantified using ODYSSEY Infrared Imaging System (LI-COR Biosciences). Signals were quantified by Image Studio Lite software (LI-COR Biosciences). Note that some proteins bands were obtained as a result of stripping (Stripping buffer, Pierce, IL, USA) and reblotting. Quantifications were normalized against loading controls ( $\beta$ -actin or Tubulin) or REVERT<sup>TM</sup> total protein staining (LI-COR Biosciences).

### Trx80 competitive assay

To confirm the specificity of the 27–30 kDa band detected by the Trx80 antibody, membranes were stripped and re-incubated with a mix of Trx80 abs and 10  $\mu$ M high Trx80 recombinant peptide.

### Trx80 ELISA

Authors followed the protocol previously described by Pekkari et al. [8]. For fly samples, 20 fly heads per group were homogenized in PBS based buffer.

Fifty micrograms of protein was applied for measurement in cells.

### Amyloid-beta 1-42 ELISA

Human A $\beta_{42}$  levels from SH-SY5Y- cells and fly brains were measured by hA $\beta_{1-42}$  ELISA (Wako Chemicals). For A $\beta_{42}$  ELISA of fly samples, proteins were extracted from 20 fresh brains per group. Three different fractions were isolated, as described by Iwata and cols [14].

### *Drosophila melanogaster* autophagy PCR array

RNA extraction from a pull of 100 brains per group was performed with RNeasy Microarray Tissue Mini kit (Qiagen). Five hundred nanograms of RNA was used for cDNA synthesis by RT [2] First Strand Kit (Qiagen). PCR was run following the manufacturer's instructions. Results were analyzed using RT [2]-Profiler Data-Analysis web-platform (raw data can be provided). All samples passed genomic DNA contamination test.

### Real-time quantitative PCR

mRNA was isolated from groups of ten fly brains. SYBRGreen-PCR Master Mix (Applied Biosystems), plus 10 ng cDNA, and 100 nM primer pair were used. Samples were analyzed with a 7500 Fast Real-Time PCR system (Applied Biosystem).  $2^{-\Delta\Delta C_t}$  method was used for result analysis [15].  $\alpha$ Tub84B was used as a housekeeping gene.

### Immunofluorescence

Fly brains or SH-SY5Y cells were fixed in 4% paraformaldehyde for 20 min followed by permeabilization and washing steps (0.2% Triton in PBS). Then, 5% BSA Blocking buffer was incubated 1 h at RT. As primary antibodies, we used Anti-A $\beta_{42}$  (JNKI, provided by Näslund [16, 17]) incubated overnight at +4 °C. Thereafter, brains were washed three times and incubated overnight with secondary antibodies AlexaFluor633 (Life Technologies) for fly samples and AlexaFluor488 for SH-SY5Y cells. Primary antibody was omitted as a negative control. Confocal imaging was performed with Zeiss LSM 510 META system. Image analysis was performed using Image J2.

## Results

### Transgenic *Drosophila melanogaster* models

We generated *Drosophila melanogaster* models over-expressing human Trx80 and human A $\beta_{42}$  (Fig. 1a).



Trx80- $A\beta_{42}$  co-expressing flies (Elav- $A\beta_{42}$  + Trx80) showed similar Trx80 or  $A\beta_{42}$  expression as single transgenic flies (Elav-Trx80 and Elav- $A\beta_{42}$ ) (Fig. 1b).

Western Blots and ELISA were performed to confirm whether the RT-PCR results were reflected on protein levels. Higher Trx80 levels were found in Elav-Trx80 compared with Elav-WT and Elav- $A\beta_{42}$  + Trx80 flies (Fig. 1c and Supplementary Fig. 1A, B). Some Trx80 signal was detected in Elav-WT and Elav- $A\beta_{42}$  flies, suggesting some off-target binding.

ELISA confirmed this result with fly head extracts of 5, 20, and 30-day-old flies (Fig. 1d). Trx80 levels were higher in Elav-Trx80 ( $19.9 \pm 2.2$  ng/brain) compared with Elav-WT ( $6.6 \pm 1.5$  ng/brain) and Elav- $A\beta_{42}$  + Trx80 flies ( $9.1 \pm 1.9$  ng/brain). Trx80 levels were also significantly higher in Elav- $A\beta_{42}$  + Trx80 compared with Elav-WT. Trx80 levels in all fly groups were not affected by age (Fig. 1d, e). However, it is important to note that Elav- $A\beta_{42}$  + Trx80 flies and WT flies showed similar Trx80 levels at 20 days.

### Trx80 inhibits $A\beta_{42}$ accumulation in vivo

As reported in vitro [12], we detected non-amyloid aggregates in  $A\beta_{42}$  expressed fly brains, similar to diffuse plaques (Supplementary Fig. 1C). Elav- $A\beta_{42}$  flies show  $A\beta_{42}$  deposits in different brain regions (Fig. 1f, g, red staining) [18]. These deposits were increased with age (5-day-old vs 30-day-old Elav- $A\beta_{42}$  flies; Fig. 1f–h) and we found significant differences between Elav-WT and Elav- $A\beta_{42}$  flies in an age-dependent manner ( $*p < 0.05$ ,  $**p < 0.01$ ).

In Elav- $A\beta_{42}$  + Trx80 flies,  $A\beta_{42}$  immunoreactivity was significantly lower than in Elav- $A\beta_{42}$  flies at 5 ( $\#p < 0.05$ ) and 30 days ( $\#\#p < 0.01$ ). Quantification software was used as shown in supplementary Fig. 1D.

Brains were also stained with DAPI (Fig. 1f, g and Supplementary Fig. 1C, blue staining).

We next analyzed fly brain homogenates by Western Blot and ELISA. Extracts from 30-day-old flies were blotted using; 6E10 (which recognizes the N-terminal area of  $A\beta_{42}$ ), and JNK1 that recognizes the C-terminal domain ( $A\beta_{42}$ -cterm) [16]. ANOVA statistical test was applied ( $*p < 0.01$ ) to analyze the signal from 4 kDa band.  $A\beta$  monomer levels were significantly higher in  $A\beta_{42}$  expressing flies (Elav- $A\beta_{42}$ ) compared with Elav-WT ( $*p < 0.05$ ).  $A\beta_{42}$  levels were significantly lower in Elav- $A\beta_{42}$  + Trx80 flies compared with Elav- $A\beta_{42}$  flies ( $\&p < 0.05$ ). Similar results were obtained using both antibodies (Fig. 2a, b).

In addition, a quantification of  $A\beta_{42}$  by ELISA was performed in brain homogenates from flies 5, 20, and 30 days old in three different solubility fractions: extracted in TBS (soluble forms of  $A\beta_{42}$ ), Guanidine Hydrochloride (GuHCl,  $A\beta_{42}$  big oligomers and small fibrils), and 70% Formic acid (FA, fibrillar  $A\beta_{42}$ ) [14].

In TBS soluble fractions (Fig. 2c and Supplementary Fig. 1e), we detected an age-dependent significant decrease of  $A\beta_{42}$  in Elav- $A\beta_{42}$  flies ( $\#p < 0.05$ ). Expression of Trx80 caused a significant reduction of  $A\beta_{42}$  in Elav- $A\beta_{42}$  + Trx80 flies compared with Elav- $A\beta_{42}$  in all ages ( $\&p < 0.01$ ).

In GuHCl-soluble fractions (Supplementary Fig. 1E), we detected increased levels of  $A\beta_{42}$  in  $A\beta_{42}$  expressing flies (Elav- $A\beta_{42}$  and Elav- $A\beta_{42}$  + Trx80) compared with Elav-WT ( $*p < 0.05$ ). Trx80 overexpression did not reduce GuHCl-soluble  $A\beta_{42}$  levels.

In FA fractions we found an age-dependent ( $\#p < 0.05$ ) increase in  $A\beta_{42}$  levels in Elav- $A\beta_{42}$  fly brains ( $*p < 0.01$ ). Also, Elav- $A\beta_{42}$  + Trx80 flies showed significantly reduced  $A\beta_{42}$  levels compared with Elav- $A\beta_{42}$  flies in all ages ( $\&p < 0.01$ ) (Fig. 2d and Supplementary Fig. 1E).

The results obtained for total  $A\beta_{42}$  levels (sum of TBS + GuHCl + FA fractions) in each fly strain by age (Fig. 2e), support those using separate fractions. Extracts from Elav- $A\beta_{42}$  flies showed significantly higher  $A\beta_{42}$  levels ( $158 \pm 5$  pg per fly brain) than Elav- $A\beta_{42}$  + Trx80 ( $64 \pm 3$  pg,  $\&p < 0.01$ ) and Elav-WT flies ( $20 \pm 2$  pg,  $*p < 0.01$ ). A summary of the ELISA results is shown in Supplementary Fig. 1E.

### Trx80 protects from $A\beta_{42}$ -induced phenotype

To study if the effect of Trx80 on  $A\beta_{42}$  levels would modify the phenotype of the fly, we performed a longevity study using 100 flies per group (Fig. 3a). As previously described by Hermansson et al. [11, 19], Elav- $A\beta_{42}$  flies had a significantly shorter life span (median: 34 days) compared with Elav-WT flies (median: 52 days) ( $p < 0.0001$ ). In contrast, flies expressing both Trx80 and  $A\beta_{42}$  had similar lifetime expectancy (Elav- $A\beta_{42}$  + Trx80 median: 51 days) as Elav-WT flies, and significantly higher than  $A\beta_{42}$  expressing flies (Elav- $A\beta_{42}$  + Trx80 vs Elav- $A\beta_{42}$ ;  $p < 0.0001$ ). Trx80-overexpressing flies had similar life expectancy as Elav-WT flies (Elav-Trx80 median: 53 days).

Locomotor activity was also assessed using 20-day-old flies (Fig. 3b). The percentage of flies climbing was significantly smaller for Elav- $A\beta_{42}$  (22%  $\pm 7$ ) compared with Elav-WT (53%  $\pm 9$ ) ( $*p < 0.0001$ ) (Fig. 3b). Trx80 expression significantly improved the  $A\beta_{42}$ -induced phenotype and the flies that were able to climb in the Elav- $A\beta_{42}$  + Trx80 group (52%  $\pm 9$ ) were significantly higher ( $\&p < 0.01$ ) than Elav- $A\beta_{42}$  and similar to Elav-WT.

### Trx80 stimulates autophagy

Previous studies using  $A\beta_{42}$  expressing *Drosophila* have been successful in preventing a harmful phenotype co-expressing another protein [11, 19]. This effect has been attributed to a delay in  $A\beta_{42}$  aggregation or an effect on brain  $A\beta_{42}$  distribution. In Trx80 and  $A\beta_{42}$  co-expressing

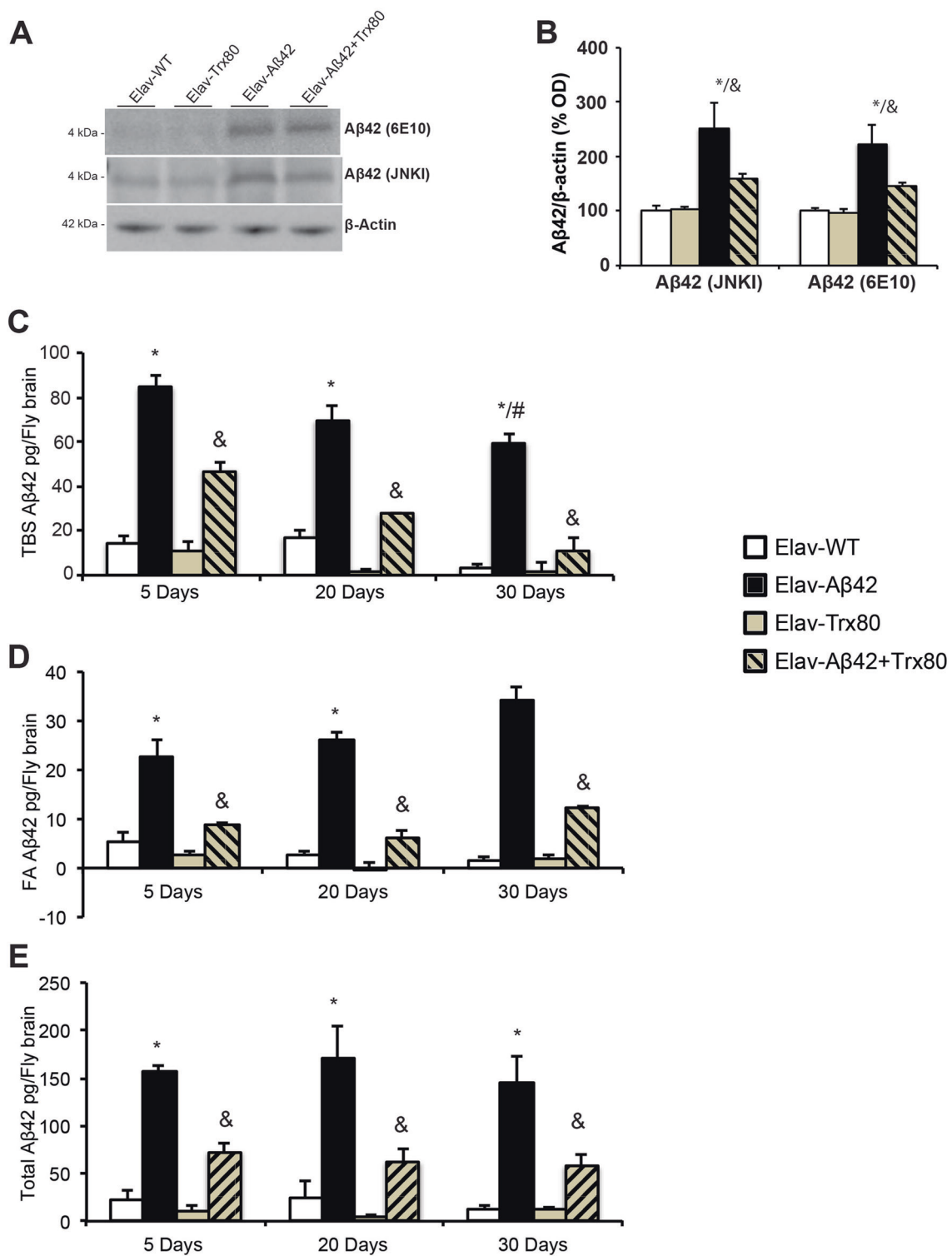


**Fig. 2** Trx80 overexpression reduces time-dependent increase of Aβ<sub>42</sub> levels and prevents Aβ<sub>42</sub> deposition in the brain of Aβ<sub>42</sub>-Trx80 co-expressing flies. **a** Representative Aβ<sub>42</sub> blots of all four fly genotypes with two different anti-Aβ<sub>42</sub> antibodies (6E10 and Aβ<sub>42</sub>-cterm JNK1). **b** Bar graph show the quantification of the Aβ<sub>42</sub> blots with data normalized to β-actin and presented as percentage of values for Elav-WT flies. Results are expressed as mean ± SD. Statistical analysis was performed by two-way ANOVA (\**p* < 0.01) and Bonferroni multiple

comparisons (Aβ<sub>42</sub> vs Aβ<sub>42</sub>-Trx80, &*p* < 0.01). (*n* = 3). **c** TBS soluble Aβ<sub>42</sub> (TBS fraction) levels in 5, 20, and 30-day-old flies. **d** Fibrillar Aβ<sub>42</sub> (Formic Acid, FA, fraction) levels in 5, 20, and 30-day-old flies. **e** Total Aβ<sub>42</sub> ELISA measurement (sum of all fractions) by age for all four groups. In **d-f** Aβ<sub>42</sub> levels are presented as pg per fly brain and results are expressed as mean ± SD. Two-way ANOVA (\**p* < 0.01) was performed together with Bonferroni multiple comparison (Aβ<sub>42</sub> vs Aβ<sub>42</sub>-Trx80, &*p* < 0.01) (5 days Aβ<sub>42</sub> vs 30 days Aβ<sub>42</sub>, #*p* < 0.05 (*n* = 3)

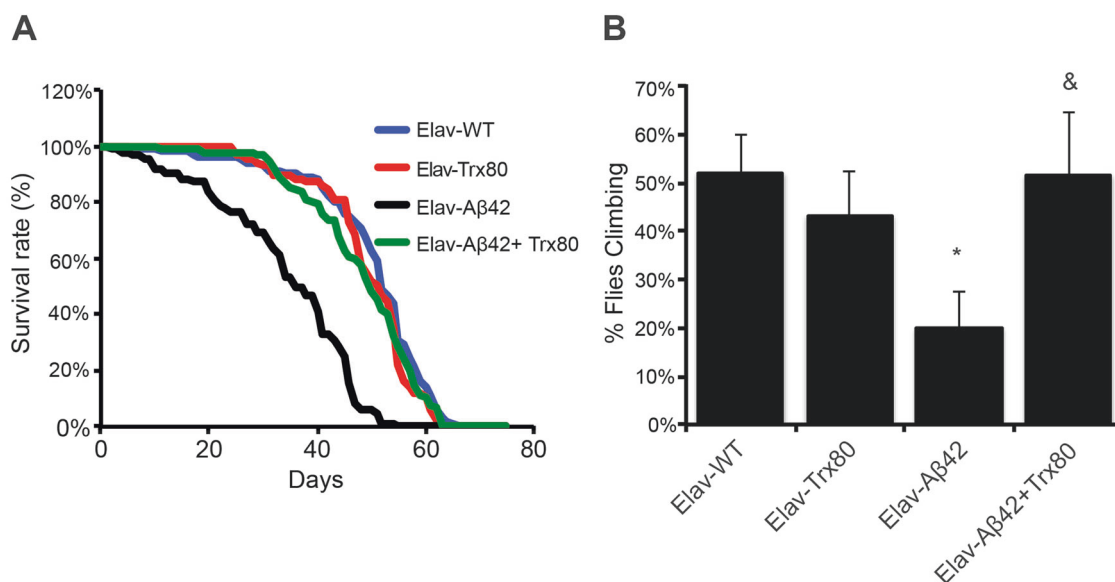


**Fig. 3** Trx80 overexpression prevents A $\beta_{42}$  induced longevity and locomotor decline. **a** A survival plot showing the fraction of 100 flies over time for WT flies and flies expressing Trx80, A $\beta_{42}$ , or both. The plots were calculated using the Kaplan–Meier method. Differences between groups were calculated using the log-rank test. Bonferroni correction was applied for multiple comparisons ( $n = 100$ ).

**b** Locomotor activity behavioral test for all fly genotypes. 20 day-old flies were used for climbing assay. Data are expressed as the percentage of flies passing for each group. A total of 50 flies of each genotype were measured 5 times for each fly. Two-way ANOVA ( $*p < 0.001$ ) was performed together with Bonferroni multiple comparison (A $\beta_{42}$  vs A $\beta_{42}$ -Trx80,  $^{\&}p < 0.01$ ). Values are expressed as mean  $\pm$  SD ( $n = 50$ )

flies, we instead observed a significant decrease of A $\beta_{42}$  pathology (Fig. 2a–f). As a possible explanation, Trx80 could facilitate A $\beta_{42}$  degradation. One of the main cellular pathways involved in the degradation of protein aggregates is macroautophagy (hereafter referred as autophagy [20]) a mechanism that was shown to be impaired in AD [21]. To explore whether the positive effects of Trx80 on A $\beta_{42}$  accumulation and A $\beta_{42}$ -related phenotype could be by regulating autophagy, we used an RT<sup>2</sup> Profiler PCR Array and measured the expression of 84 autophagy-related genes in fly brain homogenates. The expression of these genes was related to *Act42A*, *GAPDH*, *RpL32* housekeeping genes and the  $2^{-\Delta C_t}$  values were calculated. These values, showing relative expression levels, are presented as a heat map (Fig. 4a). Data are expressed as relative expression levels in Elav-WT flies and presented as fold changes (Fig. 4b). Expressions of some genes, including AMP-activated protein kinase alpha (*AMPK $\alpha$* ), Autophagy protein 2, 4a, 4b, 8a, 8b (*Atg2*, *Atg4a*, *Atg4b*, *Atg8a*, *Atg8b*), *PI3K59F*, and Draper (*drpr*), were found significantly increased in Elav-Trx80 compared with Elav-WT flies. Similar results were seen when comparing Elav-A $\beta_{42}$  + Trx80 with Elav-A $\beta_{42}$  flies (Fig. 4b).

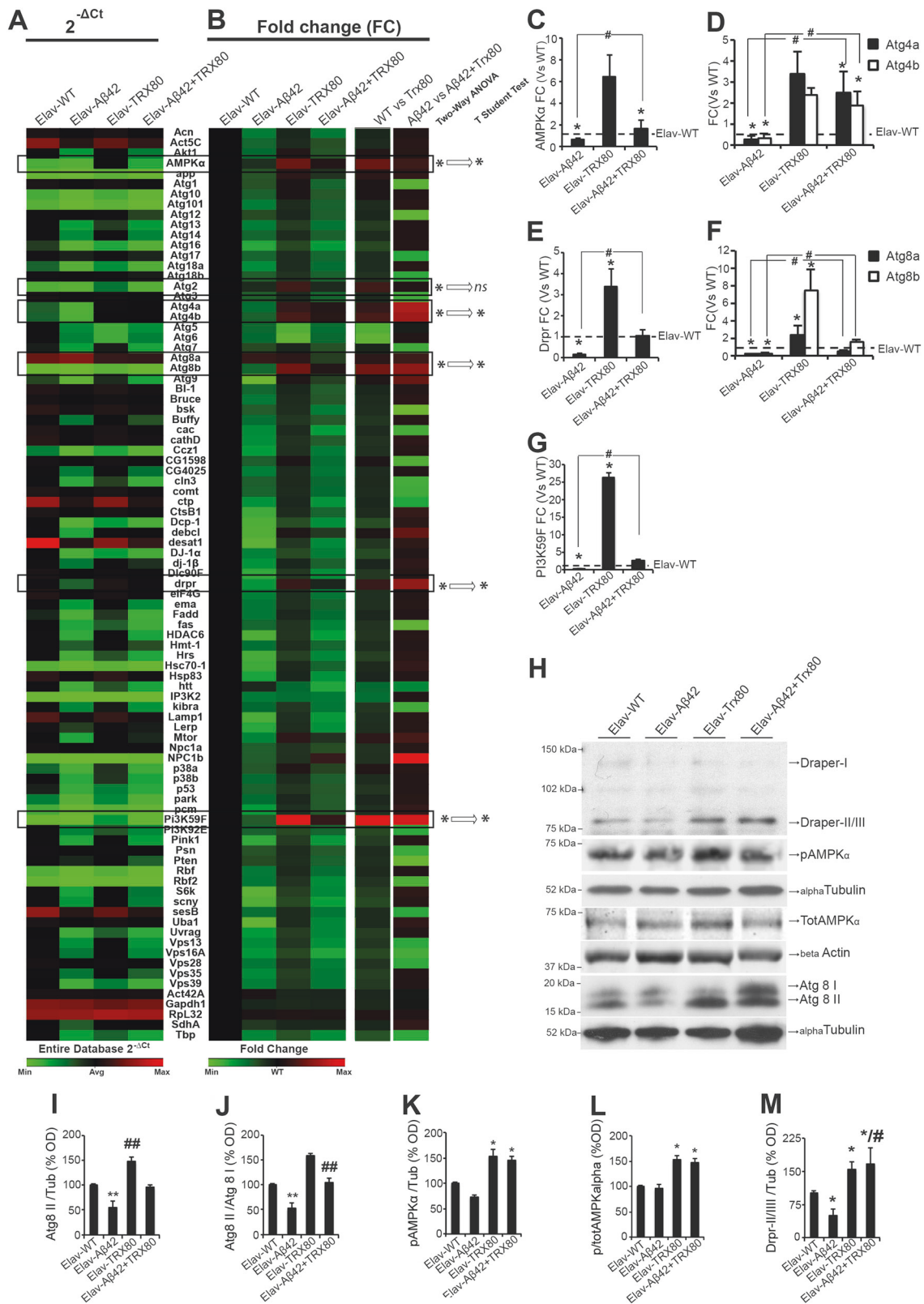
In Fig. 4c–g, fold changes are represented to respective Elav-WT expression. The expressions of *AMPK $\alpha$* , *Atg4a*, *Atg4b*, *Atg8a*, *Atg8b*, *PI3K59F* (*Drosophila* ortholog of human VPS34), and *drpr* were found a significantly reduced in Elav-A $\beta_{42}$  flies compared with Elav-WT ( $*p < 0.01$ ). In contrast, Trx80 expression in Elav-Trx80 flies results in a

significant increase in these genes compared with Elav-WT ( $*p < 0.01$ ). Moreover, Elav-A $\beta_{42}$  + Trx80 flies show increased expression of *AMPK $\alpha$* , *Atg8a*, *Atg8b*, and *drpr* compared with Elav-A $\beta_{42}$  flies ( $^{\#}p < 0.01$ ).

Effects of the selected genes were further analyzed at protein level (Fig. 4h). *Atg8* is the *Drosophila* ortholog of mammalian LC3. Initially, *Atg8* is unlipidated (*Atg8-I*), but induction of autophagy promotes its lipidation to *Atg8-II*, which is important for autophagosome formation [22] and autophagic flux [23]. *Atg8-I* levels were not altered by A $\beta_{42}$  or Trx80 expressions (Supplementary Fig. 2A). However, *Atg8-II* levels were significantly lower in Elav-A $\beta_{42}$  ( $**p < 0.01$ ) and significantly increased in Elav-Trx80 flies (Elav-WT vs Elav-Trx80,  $**p < 0.01$ , Fig. 4i). Elav-A $\beta_{42}$  + Trx80 showed significantly higher *Atg8-II* expression compared with Elav-A $\beta_{42}$  ( $^{\#\#}p < 0.01$ , Fig. 4i). Analysis of *Atg8-II/Atg8-I* ratios showed similar results (Fig. 4j) than those obtained for *Atg8-II* (Fig. 4i).

*AMPK $\alpha$* , a regulator of autophagy, is activated by phosphorylation [24, 25]. No significant differences in total *AMPK $\alpha$*  levels were detected among the different groups (Supplementary Fig. 2b). However, we detected an induction of the *AMPK $\alpha$*  phosphorylation in Trx80 flies (Elav-Trx80 and Elav-A $\beta_{42}$  + Trx80,  $*p < 0.05$ ) and on phospho-*AMPK $\alpha$*  /total*AMPK $\alpha$*  ratio (Fig. 4l) compared with non-Trx80 expressing flies (Fig. 4k).

The cell-surface engulfment receptor Draper is the *Drosophila* ortholog of human MEGF-10. Draper I, II, and III, are different isoforms of the same gene [26]. No changes



were detected in Draper I among the groups (Supplementary Fig. 2C). Draper II and III are difficult to separate on SDS-PAGE gel [27] (Fig. 4h), thus the combined band was

quantified (Fig. 4m). Brains from Elav-A $\beta_{42}$  flies showed significantly lower expression of Draper II/III than those from Elav-WT flies ( $*p < 0.05$ ). Trx80 expression



◀ **Fig. 4** Trx80 and A $\beta_{42}$  overexpression alter the autophagy pathway expression profile in *Drosophila Melanogaster* at mRNA and protein level. **a**  $2^{-\Delta Ct}$  based heatmap showing the autophagy-related gene expression profile of all experimental groups. Scale bar identifies green (value = 0) as low expressed genes and red (value = 4) as high expressed genes. **b** Heatmap based on fold change compared to Elav-WT, showing the autophagy-related gene expression profile of all experimental groups. Scale bar identifies green (value = 0) as lowly expressed genes and red (value = 4) as highly expressed genes. Fold change heatmap WT vs Trx80, Elav-WT as reference. Fold change heatmap A $\beta_{42}$  vs A $\beta_{42}$ -Trx80, Elav-A $\beta_{42}$  as reference. Two-way ANOVA was performed for each gene ( $n = 3$ ) ( $*p < 0.05$ ), followed by Student's  $t$ -tests of the most relevant comparisons (Elav-WT vs Elav-Trx80 and Elav-A $\beta_{42}$  vs Elav-A $\beta_{42}$ /Trx80) ( $*p < 0.01$ ). Statistically significant autophagy genes were selected as hits for further analysis. Histograms show differential expression of (c) AMPK $\alpha$  (d) Atg4a and Atg4b (e) Draper (Drpr) (f) Atg8a and Atg8B and (g) PI3K59F with data as fold changes to levels seen in Elav-WT. Two-way ANOVA was performed for all of them ( $*p < 0.05$ ) followed by Bonferroni posthoc analysis for the specific comparisons of interest (A $\beta_{42}$  vs A $\beta_{42}$ /Trx80;  $\#p < 0.01$ ) ( $n = 3$ ). **h** Representative immunoblots of Draper (Drpr), phospho-AMPK, total AMPK, alpha-Tubulin and Atg8 in all four fly genotypes. Levels of  $\alpha$ -tubulin were used as loading controls to normalize quantifications of, (i) Atg8-II, (j) Atg8-II/I ratio, (k) Phospho-Thr207-AMPK $\alpha$ , (l) AMPK $\alpha$  ratio, (m) Drpr II and III. Results are expressed as mean  $\pm$  SD with data expressed as percentage of levels in Elav-WT flies. Two-way ANOVA ( $**p < 0.01$ ) was performed together with Bonferroni multiple comparison (A $\beta_{42}$  vs A $\beta_{42}$ /Trx80;  $\#p < 0.01$ ). Two-way ANOVA was performed together with Bonferroni multiple comparison ( $*p < 0.05$   $**p < 0.01$  show significances against WT) (A $\beta_{42}$  vs A $\beta_{42}$ /Trx80;  $\#p < 0.01$ ). ( $*p < 0.05$ ) ( $n = 3$ )

significantly enhanced Draper II/III levels when expressed alone ( $*p < 0.05$ ). Flies co-expressing Trx80 and A $\beta_{42}$  showed similar Draper II/III levels than WT and higher than flies expressing only A $\beta_{42}$  ( $\#p < 0.05$ ) (Fig. 4m).

### Trx80 lowers A $\beta_{42}$ levels via autophagy in human neuroblastoma cells

We next explored if those effects seen in our *Drosophila melanogaster* could be reproduced in human cells. For that, we used a Trx80-overexpressing SH-SY5Y cell line (SH-Trx80) and their respective control cells (SH-SY5Y with empty vector). As seen in Supplementary Fig. 3A, C, Trx80 levels were significantly higher in SH-Trx80 cells compared with controls. The specificity of the Trx80 immunoreactive bands was confirmed by a competitive assay as described in "Material and methods". The immunocytochemical analysis showed that cells overexpressing Trx80 presented significantly lower A $\beta_{42}$  staining than control cells (Fig. 5a, b;  $**p < 0.01$ ). Since Trx80 is also secreted to the extracellular space, we quantified A $\beta_{42}$  levels in cell lysates and medium by ELISA. SH-Trx80 cells showed significantly lower A $\beta_{42}$  levels in both cell lysates ( $**p < 0.01$ ) and media ( $*p < 0.05$ ) as compared with control cells (Fig. 5c).

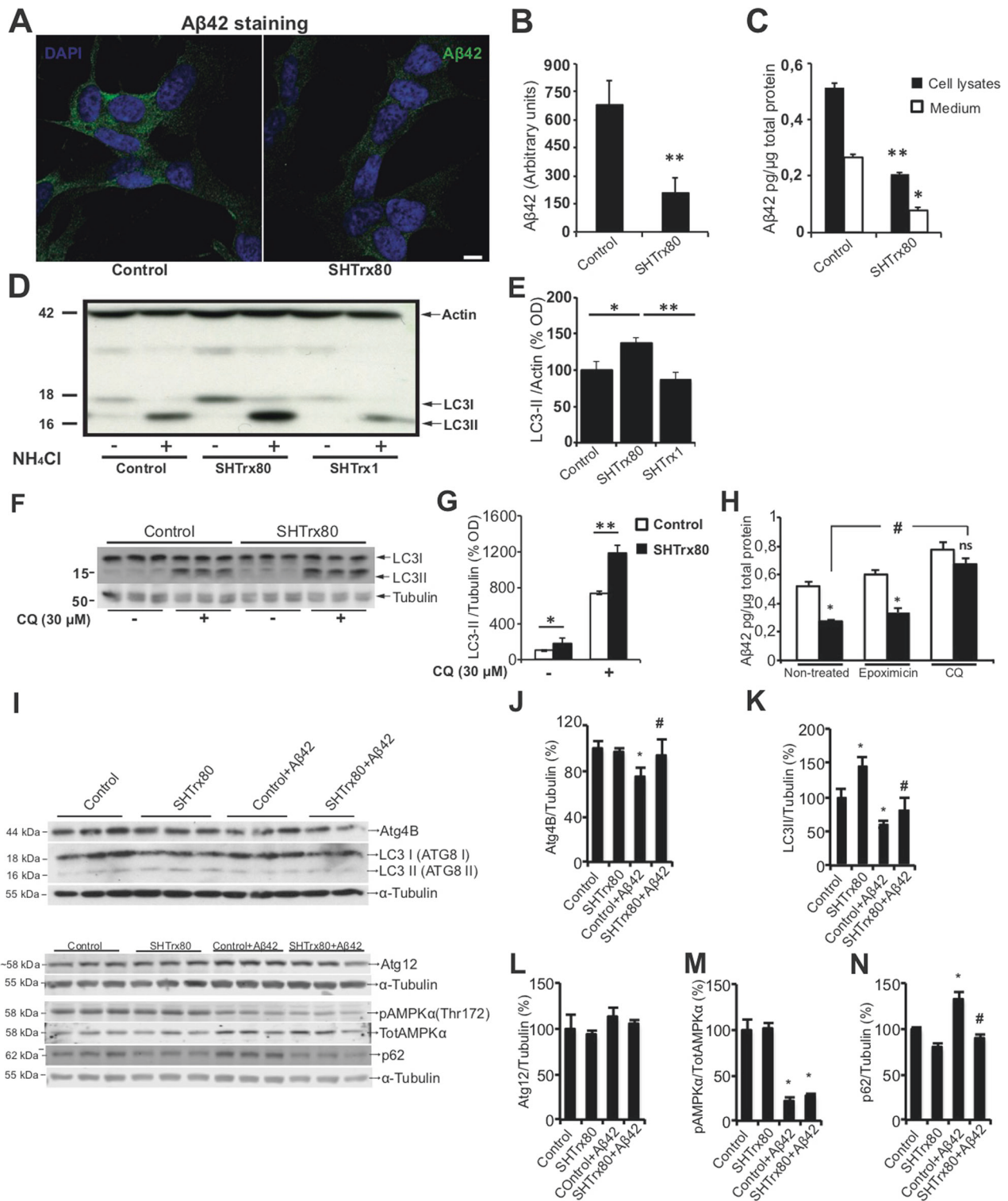
A $\beta$  can be intracellularly degraded by proteases [28], autophagy [29], or the ubiquitin-proteasome system [30]. We checked if the expression of two main A $\beta_{42}$  degrading proteases, insulin-degrading enzyme (IDE) [31, 32] and neprilysin (NEP) [14, 33], were altered by Trx80 overexpression. As seen in Supplementary Fig. 3D–F, Trx80 overexpression did not change IDE or NEP levels.

To test if Trx80 affects the ubiquitin-proteasome system, cells were treated with the proteasome inhibitor EPOX and the amount of ubiquitinated protein levels was quantified. As expected, a significant increase in ubiquitinated proteins was detected in EPOX treated samples compared with non-treated groups. As seen in Supplementary Figs. 3G and 4H, Trx80 overexpression did not affect the levels of ubiquitinated proteins.

In order to study the autophagic flux, we next analyzed the effects of Trx80 overexpression on LC3 levels in cells treated with or without NH $_4$ Cl, an inhibitor of endosome-lysosome system acidification to prevent autophagosome protein degradation [20]. Empty vector (control) cells and cells overexpressing full-length Trx1 (SH-Trx1) were used as controls [34]. We found that LC3II levels were significantly higher in SH-Trx80 cells compared with both control ( $*p < 0.05$ ) and SH-Trx1 cells ( $**p < 0.01$ ) (Fig. 5d, e). These effects on LC3 were confirmed when using Chloroquine (CQ, 30  $\mu$ M) as alternative autophagic flux blocker (Fig. 5f, g). NH $_4$ Cl treatment induced an increase of LC3I levels on SH-Trx80 cells, an effect that was not seen by CQ treatment.

We also measured A $\beta_{42}$  levels by ELISA in untreated, EPOX, and CQ treated in control and SH-Trx80 cells (Fig. 5h). This allowed us to measure the direct impact of each pathway on A $\beta_{42}$  clearance. As reported above, untreated SH-Trx80 cells showed lower levels of A $\beta_{42}$  than controls. Blockage of the ubiquitin-proteasome system pathway with EPOX did not alter the A $\beta_{42}$  levels seen in untreated cells. However, inhibition of autophagy with CQ, resulted in a remarkable increase of A $\beta_{42}$  levels in both controls and SH-Trx80 cells.

To elucidate the effects of Trx80 and A $\beta_{42}$  on autophagy, we studied the effects of recombinant A $\beta_{42}$  in macroautophagy. SH-Trx80 cells were pre-treated with A $\beta_{42}$  (500 nM, 6 h) (SH-Trx80 + A $\beta_{42}$ ) and levels of Atg4B, LC3I, and LC3II, Atg 12, pAMPK, totalAMPK and p62 were measured. Levels of Atg4B (responsible for cleavage and activation of LC3) were lower in A $\beta_{42}$  treated cells than in controls ( $*p < 0.05$ ) (Fig. 5i, j and Supplementary Fig. 4). This A $\beta_{42}$ -mediated effect was not seen in cells overexpressing Trx80 ( $\#p < 0.01$ ). Consequently, Trx80 overexpression induced an increase in LC3II levels compared with controls ( $*p < 0.01$ ), and also in A $\beta_{42}$  treated cells ( $\#p < 0.05$ ) (Fig. 5k). In addition to LC3 [35],



Atg12 also participates in the conjugation pathways of autophagosomes. Overexpression of Trx80 or exogenous addition of Aβ<sub>42</sub> did not modify Atg12 levels (Fig. 5I). Aβ<sub>42</sub> treatment significantly decreased AMPK phosphorylation (\**p* < 0.01) by Trx80 overexpression did not affect levels of

AMPK phosphorylation. p62 participates in the recruitment of ubiquitinated proteins to autophagosomes [36]. As seen in Fig. 5n, Aβ<sub>42</sub> treatment resulted in higher p62 levels in control cells (\**p* < 0.01), but not in Trx80-overexpressing cells (#*p* < 0.01).

◀ **Fig. 5** Trx80 overexpression enhances A $\beta_{42}$  clearance in a mammalian neuroblastoma cell line (SH-SY5Y) through autophagy-lysosomal pathway regulation. **a** Confocal microscopy images of cultured SH-SY5Y and SH-Trx80 cells using anti-A $\beta_{42}$  (green) and DAPI (blue). Scale bar: 20  $\mu$ m. **b** Quantification of A $\beta_{42}$  immunofluorescence in Control (SH-SY5Y empty vector) and SH-Trx80 cells. Values are expressed as mean  $\pm$  SD. Data are presented as arbitrary units (a.u) ( $*p < 0.05$ , Man-Whitney test,  $n = 10$ ). **c** Quantitative specific A $\beta_{42}$ -ELISA to measure A $\beta_{42}$  protein levels in cell lysates and cell medium (24 h conditioned medium) of Control and SH-Trx80 cells. Values are expressed as mean  $\pm$  SD with data as A $\beta_{42}$  pg per  $\mu$ g of total protein. Statistical analysis was performed by Student's *t*-test ( $**p < 0.01$ ,  $n = 4$ ). **d** Representative picture from Western blot analysis of LC3 levels in control cells overexpressing either Trx80 or Trx1. Cells transfected with an empty plasmid were used as Control. Cells were treated with or without NH $_4$ Cl indicated by (+) or (–) respectively ( $n = 5$ ). **e** Quantification of band intensities in **d**. **f** Representative picture from Western blot analysis of LC3 levels in control and SH-Trx80 cells. Cells were treated with or without 30  $\mu$ M, 6 h Chloroquine (CQ) indicated by (+) or (–) respectively ( $n = 6$ ). **g** Quantification of band intensities in **f**. All results are expressed as mean  $\pm$  SD. Statistical analysis was performed by One-way ANOVA ( $*p < 0.01$ , control vs Trx80  $**p < 0.01$ , Bonferroni's multiple comparison test). **h** Quantitative specific A $\beta_{42}$ -ELISA to measure A $\beta_{42}$  protein levels in Control and SH-Trx80 cells untreated or treated with Epoximicin, specific Ubiquitin-proteasome system inhibitor (250 nM), or Chloroquine (CQ, 30  $\mu$ M). Values are expressed as mean  $\pm$  SD. Data are presented as A $\beta_{42}$  pg per  $\mu$ g of total protein. Statistical analysis was performed by Student's *t*-test ( $**p < 0.01$ ,  $n = 4$ ). **i** Representative pictures from Western blot analysis of Atg4B, LC3 I, LC3 II, Atg12, Phospho-Thr-AMPKalpha, AMP-Kalpha, and p62 levels of SH-SY5Y cells overexpressing Trx80 (SH-Trx80) and SH-SY5Y empty vector (controls) treated or not with recombinant A $\beta_{42}$  (500 nM, 6 h). Histograms show levels of Atg4B (**j**), LC3 II (**k**), Atg12 (**l**), Phospho-Thr172-AMPKalpha, phospho/total AMPKalpha ratio (**m**), and p62 (**n**). Values are expressed as mean  $\pm$  SD with data as percentage of control values. Statistical analysis was performed by two-way ANOVA ( $*p < 0.01$ ) and Bonferroni multiple comparison test (A $\beta_{42}$  vs A $\beta_{42}$  + Trx80,  $^{\#}p < 0.01$ ) ( $n = 3$ )

## Discussion

Trx80 was initially described as a proinflammatory peripheral cytokine secreted by immune cells [37, 38]. We previously reported the presence of Trx80 in the brain and found that the levels of this peptide were dramatically reduced in AD. In addition, we demonstrated that Trx80 inhibits A $\beta$  aggregation and toxicity in vitro [10]. In the present study, we investigated the effects of Trx80 on A $\beta$  toxicity in vivo using *Drosophila melanogaster* models. We found that expression of human A $\beta_{42}$  in the fly brain causes progressive age-dependent depositions of this peptide and causes reduced life span and impaired locomotor activity [11, 39]. We showed that soluble A $\beta_{42}$  is highly expressed in young flies, while age leads to a progressive insoluble/fibrillar A $\beta_{42}$  accumulation. In A $\beta_{42}$  and Trx80 co-expressing flies, A $\beta_{42}$  accumulation was drastically reduced, and the A $\beta_{42}$  depending phenotype in early mortality and locomotor activity was reversed.

Elav-A $\beta_{42}$  + Trx80 showed similar Trx80 mRNA expression, but lower Trx80 and A $\beta_{42}$  protein levels than Elav-Trx80 flies. This suggests that Trx80 could play a role in A $\beta_{42}$  metabolism. In support of this idea, overexpression of Trx80 also results in decreased intracellular levels of A $\beta_{42}$  in neural mammalian cells.

Three main intracellular pathways have been described for metabolism and removal of A $\beta$ : A $\beta$  degrading proteases [28, 31, 33], the ubiquitin-proteasome system [40] and autophagy [41, 42]. Our results seemingly exclude the involvement of Trx80 on A $\beta$  metabolism by the two first degrading systems. In SH-SY5Y human cells, Trx80 did not induce the expression of main A $\beta$  degrading proteases, and it did not alter general ubiquitination processes. Furthermore, ubiquitin-proteasome system inhibition did not alter Trx80 effects on A $\beta_{42}$  levels. On the other hand, we showed that Trx80 induces the expression of key proteins for the induction of autophagy in *Drosophila* and in mammalian neuronal cells. We showed a Trx80-mediated increase of Atg4B, and markers for autophagosome formation as LC3a II and LC3b II [43]. We also found that a trx80-mediated induction of Drpr expression, a *Drosophila* homolog to human MEGF-10, which is a cell-surface receptor required for the recognition and engulfment of apoptotic cells, glial clearance of axon fragments and dendritic pruning [44]. Although a direct link between autophagy and MEGF-10 has never been found in the adult brain, Drpr enhances autophagy signaling in salivary glands during development [45] and is required for autophagy during cell death [46]. Importantly, when autophagy was chemically blocked, Trx80 effects on A $\beta_{42}$  levels were not shown. Together, our results in human cells and in vivo strongly suggest that Trx80-induced reduction of A $\beta_{42}$  is mediated by the enhancement of the autophagic-lysosomal pathway.

Initiation of autophagy involves the isolation and elongation of an ER-derived membrane known as phagophore. This structure then elongates into a cup-shaped structure and begins to engulf cellular material [47]. These vesicles can uptake organelles, metabolites, peptides, and misfolded proteins. Then autophagosomes fuse with lysosomes to form the autophagolysosomes, promoting the digestion of sequestered material by acidic hydrolases [48]. It has been widely accepted that abnormal autophagy is associated with A $\beta$  pathology [40, 49]. A $\beta$  is present in autophagosomes and autophagolysosomes [50] and APP and APP processing enzymes ( $\alpha$ ,  $\beta$ , and  $\gamma$ -secretases) have also been identified in these structures [51]. Moreover, an abnormal accumulation of autophagosomes and autophagolysosomes has been reported in AD [52]. In AD patients, resolution of autophagy [53] is impaired, LC3-II levels are decreased, p62 interaction with LC3-II is not effective and p62 accumulates and aggregates [54]. Binding of p62 and LC3-II targets ubiquitin-conjugated proteins for autophagosome-dependent degradation [55]. In



agreement with a previous study in an A $\beta$  mouse model [55], we show that A $\beta_{42}$  enhances p62 levels in cells. Moreover, we found that overexpression of Trx80 reverses A $\beta_{42}$  dependent p62 increase in human cells. Our results further demonstrate that Trx80 plays a role in the resolution of autophagy, increasing the expression of Atg4B and LC3II resulting in enhanced autophagolysosome formation and A $\beta_{42}$  metabolism. Interestingly, Cortes-Bratti and colleagues previously speculated that Trx80 participates in the control of intracellular infections by inducing autophagosome formation to degrade pathogens [56]. Thus, besides its chemokine activity [9], one biological function of Trx80 would be the regulation of conjugation phase of autophagy, helping cells to degrade toxic aggregates or pathogens. Supporting this idea, several other thioredoxin proteins have been shown to modulate autophagy in different models, from yeast [57] to *Caenorhabditis elegans* in models of Alzheimer's, Huntington and Parkinson's diseases [58].

In summary, we previously reported that Trx80 inhibits A $\beta$  aggregation and protects against its toxic effects in vitro [10]. Now we show that Trx80 protects against A $\beta$  toxicity in vivo and promotes A $\beta$  degradation by boosting the conjugation phase of autophagy. In a scenario of depleted Trx80, such as in AD brains [10], misfolded proteins like A $\beta$  could accumulate in oligomers and fibrils inside the neurons compromising neuronal survival and brain function. Increasing Trx80 would result in enhanced autophagic degradation of toxic A $\beta$  entities (Supplementary Fig. 5). Further studies need to be conducted in order to find the specific molecular target of Trx80 in the conjugation phase of autophagy.

The results presented in this study bring support to the function of Trx80, and therefore of Trx1 cleavage to Trx80, in the regulation of autophagy. Moreover, our findings reinforce the role of Trx80 as an endogenous agent against A $\beta$ -induced toxicity in the brain, suggesting that strategies to enhance Trx80 levels in neurons could be potentially used as treatment against AD pathology.

**Acknowledgements** We would like to acknowledge Janne Johansson for provide us the facilities of their lab and Gunnilla Westermarck for provide us the A $\beta_{42}$  overexpressing flies. This study was partially performed at the Live Cell Imaging facility of Karolinska Institutet, (Sweden).

**Funding** GGL was the recipient of the Basque Government Postdoctoral Fellowship (POS 2015-1-0028). This research was supported by the following Swedish foundations: HP was supported by The Swedish Institute Visby Program and European Social Fund's Doctoral Studies and Internationalization Programme DoRa carried out by Archimedes Foundation. Swedish Brain Power, the regional agreement on medical training and clinical research (ALF) between Stockholm County Council and Karolinska Institutet, Margaretha af Ugglas Foundation, Olle Engkvist Byggmästare Stiftelse, Gun och Bertil Stohnes Stiftelse, Loo och Hans Osterman Foundation, Karolinska Institutet fund for geriatric research, Stiftelsen Gamla Tjänarinnor,

Alzheimerfonden, the Centre for Innovative Medicine and the Jonasson center at the Royal Institute of Technology (Sweden).

**Author contributions** GGL performed the most *Drosophila* animal model experiments as well as the majority of in vitro experiments. He wrote the manuscript together with TP and ACM, collecting input from all the authors. Together with ACM and TP, he planned the experiments and analyzed the results. TP collaborated in the creation of *Drosophila* models and performed several experiments including behavioral studies. He participated also in the writing process of the manuscript. JG participated in amyloid beta 42 measurements both in vivo and in vitro models. He also participated in behavioral assays and the editing of the manuscript. JCG performed some of the in vitro experiments and participated in editing the paper. RLV participated in establishing the PCR array for the flies. Contributed to discuss results and interpretation of data. He revised the manuscript for consistency and grammar. PP participated in ELISAs measurements of Trx80 and Amyloid Beta 42. He has also contributed in writing the manuscript. CS and JP participated in the interpretation of the data as well as in the critical analysis of the results. HP helped in generating the *Drosophila* models and participated on the edition the paper. AC-M is the PI of the study. He reviewed and interpreted the results, led discussions to guide the paper scientifically and participated in the writing of manuscript.

## Compliance with ethical standards

**Conflict of interest** AC-M is currently working in Sanofi but declares no conflict of interest. The other authors have no conflict of interest to declare.

**Publisher's note** Springer Nature remains neutral with regard to jurisdictional claims in published maps and institutional affiliations.

## References

1. Nilsson P, Saido TC. Dual roles for autophagy: degradation and secretion of Alzheimer's disease A beta peptide. *Bioessays*. 2014; 36:570–8.
2. Akwa Y, Gondard E, Mann A, Capetillo-Zarate E, Alberdi E, Matute C, et al. Synaptic activity protects against AD and FTD-like pathology via autophagic-lysosomal degradation. *Mol Psychiatry*. 2017;23:1530–40.
3. Gerenu G, Martisova E, Ferrero H, Carracedo M, Rantamaki T, Ramirez MJ, et al. Modulation of BDNF cleavage by plasminogen-activator inhibitor-1 contributes to Alzheimer's neuropathology and cognitive deficits. *Biochim Biophys Acta*. 2017;1863:991–1001.
4. Finder VH, Glockshuber R. Amyloid-beta aggregation. *Neurodegener Dis*. 2007;4:13–27.
5. Epis R, Marcello E, Gardoni F, Di Luca M. Alpha, beta-and gamma-secretases in Alzheimer's disease. *Front Biosci (Sch Ed)*. 2012;4:1126–50.
6. Selkoe DJ. Alzheimer's disease: genes, proteins, and therapy. *Physiol Rev*. 2001;81:741–66.
7. Arner ES, Holmgren A. Physiological functions of thioredoxin and thioredoxin reductase. *Eur J Biochem*. 2000;267:6102–9.
8. Pekkarinen K, Gurunath R, Arner ES, Holmgren A. Truncated thioredoxin is a mitogenic cytokine for resting human peripheral blood mononuclear cells and is present in human plasma. *J Biol Chem*. 2000;275:37474–80.
9. King BC, Nowakowska J, Karsten CM, Kohl J, Renstrom E, Blom AM. Truncated and full-length thioredoxin-1 have opposing



- activating and inhibitory properties for human complement with relevance to endothelial surfaces. *J Immunol.* 2012;188:4103–12.
10. Gil-Bea F, Akterin S, Persson T, Mateos L, Sandebring A, Avila-Carino J, et al. Thioredoxin-80 is a product of alpha-secretase cleavage that inhibits amyloid-beta aggregation and is decreased in Alzheimer's disease brain. *EMBO Mol Med.* 2012;4:1097–111.
  11. Hermansson E, Schultz S, Crowther D, Linse S, Winblad B, Westermark G, et al. The chaperone domain BRICHOS prevents CNS toxicity of amyloid-beta peptide in *Drosophila melanogaster*. *Dis Model Mech.* 2014;7:659–65.
  12. Crowther DC, Kinghorn KJ, Miranda E, Page R, Curry JA, Duthie FA, et al. Intraneuronal Abeta, non-amyloid aggregates and neurodegeneration in a *Drosophila* model of Alzheimer's disease. *Neuroscience.* 2005;132:123–35.
  13. Duffy JB. GAL4 system in *Drosophila*: a fly geneticist's Swiss army knife. *Genesis.* 2002;34:1–15.
  14. Iwata N, Tsubuki S, Takaki Y, Shirohara K, Lu B, Gerard NP, et al. Metabolic regulation of brain Abeta by neprilysin. *Science.* 2001;292:1550–2.
  15. Livak KJ, Schmittgen TD. Analysis of relative gene expression data using real-time quantitative PCR and the 2<sup>-ΔΔC<sub>T</sub></sup> method. *Methods.* 2001;25:402–8.
  16. Naslund J, Haroutunian V, Mohs R, Davis KL, Davies P, Greengard P, et al. Correlation between elevated levels of amyloid beta-peptide in the brain and cognitive decline. *J Am Med Assoc.* 2000;283:1571–7.
  17. Zheng L, Calvo-Garrido J, Hallbeck M, Hultenby K, Marcusson J, Cedazo-Minguez A, et al. Intracellular localization of amyloid-beta peptide in SH-SY5Y neuroblastoma cells. *J Alzheimers Dis.* 2013;37:713–33.
  18. Ito K, Shinomiya K, Ito M, Armstrong JD, Boyan G, Hartenstein V, et al. A systematic nomenclature for the insect brain. *Neuron.* 2014;81:755–65.
  19. Poska H, Haslbeck M, Kurudenkandy FR, Hermansson E, Chen G, Kostallas G, et al. Dementia-related Bri2 BRICHOS is a versatile molecular chaperone that efficiently inhibits Abeta42 toxicity in *Drosophila*. *Biochem J.* 2016;473:3683–704.
  20. Mizushima N, Yoshimori T, Levine B. Methods in mammalian autophagy research. *Cell.* 2010;140:313–26.
  21. Nixon RA. Autophagy, amyloidogenesis and Alzheimer disease. *J Cell Sci.* 2007;120(Pt 23):4081–91.
  22. Nakatogawa H, Ichimura Y, Ohsumi Y. Atg8, a ubiquitin-like protein required for autophagosome formation, mediates membrane tethering and hemifusion. *Cell.* 2007;130:165–78.
  23. Galluzzi L, Baehrecke EH, Ballabio A, Boya P, Bravo-San Pedro JM, Cecconi F, et al. Molecular definitions of autophagy and related processes. *EMBO J.* 2017;36:1811–36.
  24. Ulgherait M, Rana A, Rera M, Graniel J, Walker DW. AMPK modulates tissue and organismal aging in a non-cell-autonomous manner. *Cell Rep.* 2014;8:1767–80.
  25. Willows R, Sanders MJ, Xiao B, Patel BR, Martin SR, Read J, et al. Phosphorylation of AMPK by upstream kinases is required for activity in mammalian cells. *Biochem J.* 2017;474:3059–73.
  26. Freeman MR, Delrow J, Kim J, Johnson E, Doe CQ. Unwrapping glial biology: Gcm target genes regulating glial development, diversification, and function. *Neuron.* 2003;38:567–80.
  27. Logan MA, Hackett R, Doherty J, Sheehan A, Speese SD, Freeman MR. Negative regulation of glial engulfment activity by Draper terminates glial responses to axon injury. *Nat Neurosci.* 2012;15:722–30.
  28. Rogeberg M, Furlund CB, Moe MK, Fladby T. Identification of peptide products from enzymatic degradation of amyloid beta. *Biochimie.* 2014;105:216–20.
  29. Caccamo A, Ferreira E, Branca C, Oddo S. p62 improves AD-like pathology by increasing autophagy. *Mol Psychiatry.* 2017;22:865–73.
  30. Hong L, Huang HC, Jiang ZF. Relationship between amyloid-beta and the ubiquitin-proteasome system in Alzheimer's disease. *Neurol Res.* 2014;36:276–82.
  31. Kurochkin IV. Insulin-degrading enzyme: embarking on amyloid destruction. *Trends Biochem Sci.* 2001;26:421–5.
  32. Qiu WQ, Folstein MF. Insulin, insulin-degrading enzyme and amyloid-beta peptide in Alzheimer's disease: review and hypothesis. *Neurobiol Aging.* 2006;27:190–8.
  33. Farris W, Schutz SG, Cirrito JR, Shankar GM, Sun X, George A, et al. Loss of neprilysin function promotes amyloid plaque formation and causes cerebral amyloid angiopathy. *Am J Pathol.* 2007;171:241–51.
  34. Akterin S, Cowburn RF, Miranda-Vizuete A, Jimenez A, Bogdanovic N, Winblad B, et al. Involvement of glutaredoxin-1 and thioredoxin-1 in beta-amyloid toxicity and Alzheimer's disease. *Cell Death Differ.* 2006;13:1454–65.
  35. Kaur J, Debnath J. Autophagy at the crossroads of catabolism and anabolism. *Nat Rev Mol Cell Biol.* 2015;16:461–72.
  36. Katsuragi Y, Ichimura Y, Komatsu M. p62/SQSTM1 functions as a signaling hub and an autophagy adaptor. *FEBS J.* 2015;282:4672–8.
  37. Pekkari K, Holmgren A. Truncated thioredoxin: physiological functions and mechanism. *Antioxid Redox Signal.* 2004;6:53–61.
  38. Couchie D, Vaisman B, Abderrazak A, Mahmood DFD, Hamza MM, Canesi F, et al. Human plasma thioredoxin-80 increases with age and in ApoE<sup>-/-</sup> mice induces inflammation, angiogenesis, and atherosclerosis. *Circulation.* 2017;136:464–75.
  39. Kumar S, Rezaei-Ghaleh N, Terwel D, Thal DR, Richard M, Hoch M, et al. Extracellular phosphorylation of the amyloid beta-peptide promotes formation of toxic aggregates during the pathogenesis of Alzheimer's disease. *EMBO J.* 2011;30:2255–65.
  40. Ihara Y, Morishima-Kawashima M, Nixon R. The ubiquitin-proteasome system and the autophagic-lysosomal system in Alzheimer disease. *Cold Spring Harb Perspect Med.* 2012;2:1–28.
  41. Ciechanover A, Kwon YT. Degradation of misfolded proteins in neurodegenerative diseases: therapeutic targets and strategies. *Exp Mol Med.* 2015;47:e147.
  42. Vilchez D, Saez I, Dillin A. The role of protein clearance mechanisms in organismal ageing and age-related diseases. *Nat Commun.* 2014;5:5659.
  43. Botti-Millet J, Nascimbeni AC, Dupont N, Morel E, Codogno P. Fine-tuning autophagy: from transcriptional to posttranslational regulation. *Am J Physiol Cell Physiol.* 2016;311:C351–62.
  44. Fullard JF, Baker NE. Signaling by the engulfment receptor draper: a screen in *Drosophila melanogaster* implicates cytoskeletal regulators, Jun N-terminal Kinase, and Yorkie. *Genetics.* 2015;199:117–34.
  45. McPhee CK, Balgley BM, Nelson C, Hill JH, Batlevi Y, Fang X, et al. Identification of factors that function in *Drosophila* salivary gland cell death during development using proteomics. *Cell Death Differ.* 2013;20:218–25.
  46. McPhee CK, Logan MA, Freeman MR, Baehrecke EH. Activation of autophagy during cell death requires the engulfment receptor Draper. *Nature.* 2010;465:1093–6.
  47. Hailey DW, Rambold AS, Satpute-Krishnan P, Mitra K, Sougrat R, Kim PK, et al. Mitochondria supply membranes for autophagosome biogenesis during starvation. *Cell.* 2010;141:656–67.
  48. Yoshimori T, Yamamoto A, Moriyama Y, Futai M, Tashiro Y. Bafilomycin A1, a specific inhibitor of vacuolar-type H<sup>(+)</sup>-ATPase, inhibits acidification and protein degradation in lysosomes of cultured cells. *J Biol Chem.* 1991;266:17707–12.
  49. Nixon RA, Yang DS. Autophagy failure in Alzheimer's disease—locating the primary defect. *Neurobiol Dis.* 2011;43:38–45.
  50. Nilsson P, Loganathan K, Sekiguchi M, Matsuba Y, Hui K, Tsubuki S, et al. Abeta secretion and plaque formation depend on autophagy. *Cell Rep.* 2013;5:61–69.

51. Yu WH, Kumar A, Peterhoff C, Shapiro Kulnane L, Uchiyama Y, Lamb BT, et al. Autophagic vacuoles are enriched in amyloid precursor protein-secretase activities: implications for beta-amyloid peptide over-production and localization in Alzheimer's disease. *Int J Biochem Cell Biol.* 2004;36:2531–40.
52. Maxfield FR. Role of endosomes and lysosomes in human disease. *Cold Spring Harb Perspect Biol.* 2014;6:a016931.
53. Chan LL, Shen D, Wilkinson AR, Patton W, Lai N, Chan E, et al. A novel image-based cytometry method for autophagy detection in living cells. *Autophagy.* 2012;8:1371–82.
54. Riley BE, Kaiser SE, Shaler TA, Ng AC, Hara T, Hipp MS, et al. Ubiquitin accumulation in autophagy-deficient mice is dependent on the Nrf2-mediated stress response pathway: a potential role for protein aggregation in autophagic substrate selection. *J Cell Biol.* 2010;191:537–52.
55. Joshi G, Gan KA, Johnson DA, Johnson JA. Increased Alzheimer's disease-like pathology in the APP/ PS1DeltaE9 mouse model lacking Nrf2 through modulation of autophagy. *Neurobiol Aging.* 2015;36:664–79.
56. Cortes-Bratti X, Basseres E, Herrera-Rodriguez F, Botero-Kleiven S, Coppotelli G, Andersen JB, et al. Thioredoxin 80-activated-monocytes (TAMs) inhibit the replication of intracellular pathogens. *PLoS ONE.* 2011;6:e16960.
57. Perez-Perez ME, Zaffagnini M, Marchand CH, Crespo JL, Lemaire SD. The yeast autophagy protease Atg4 is regulated by thioredoxin. *Autophagy.* 2014;10:1953–64.
58. Munoz-Lobato F, Rodriguez-Palero MJ, Naranjo-Galindo FJ, Shephard F, Gaffney CJ, Szewczyk NJ, et al. Protective role of DNJ-27/ERdj5 in *Caenorhabditis elegans* models of human neurodegenerative diseases. *Antioxid Redox Signal.* 2014;20:217–35.